

Spin Liquid Ground State of the $S = 1/2$ Kagome Heisenberg Model

Simeng Yan,¹ David A. Huse,^{2,3} and Steven R. White¹

¹*Department of Physics and Astronomy, University of California, Irvine, CA 92617*

²*Department of Physics, Princeton University, Princeton, NJ 08544*

³*Institute for Advanced Study, Princeton, NJ 08540*

(Dated: November 26, 2024)

Condensed matter physicists have long sought a realistic two-dimensional (2D) magnetic system whose ground state is a *spin liquid*—a zero temperature state in which quantum fluctuations have melted away any form of magnetic order. The nearest-neighbor $S = \frac{1}{2}$ Heisenberg model on the kagome lattice has seemed an ideal candidate, but in recent years some approximate numerical approaches to it have yielded instead a valence bond crystal. We have used the density matrix renormalization group to perform very accurate simulations on numerous cylinders with circumferences up to 12 lattice spacings, finding instead of the valence bond crystal a singlet-gapped spin liquid with substantially lower energy that appears to have Z_2 topological order. Our results, through a combination of very low energy, short correlation lengths and corresponding small finite size effects, a new rigorous energy bound, and consistent behavior on many cylinders, provide strong evidence that the 2D ground state of this model is a gapped spin liquid.

PACS numbers:

I. INTRODUCTION

A spin liquid (SL) is a magnetic system which has “melted” because of quantum fluctuations, even at zero temperature.¹ More precisely, it is a spin ground state with no broken symmetries, namely no preferred spin orientations, and no frozen valence bond patterns. Spin liquids, besides being exotic and novel forms of matter, have been suggested as possible routes to high temperature superconductivity,² and their unusual topological properties may be useful in building quantum computers.³ A “Holy Grail” of condensed matter physics has been to find a realistic two-dimensional (2D) spin liquid. Spin-liquid-like behavior is common in one dimension—quantum fluctuations are stronger in lower dimensions—and some systems with spatial anisotropy, in effect interpolating between one and two dimensions, are thought to be spin liquids.⁴ The strong charge fluctuations associated with being near the Mott transition, past which there are no localized spins, apparently can produce a spin liquid even without geometric frustration.⁵ Strong multispin interactions, such as ring exchanges, are associated with this regime, and these terms have been included in 2D Hamiltonians to force spin liquid ground states.⁶ Of great interest would be a spin liquid with a Hamiltonian that is isotropic in both space and spin directions, with no multispin interactions and preferably only nearest-neighbor exchange interactions on a simple lattice, where the spin liquid behavior is driven entirely by frustration. Here we present strong evidence for just such a spin liquid.

The Heisenberg $S = \frac{1}{2}$ kagome lattice model (HKLM) has long been thought to be the ideal candidate. On the experimental side, the material herbertsmithite, $\text{ZnCu}_3(\text{OH})_6\text{Cl}_2$, is a spin-1/2 kagome antiferromagnet showing spin liquid behavior.^{7–10} It is thought to be well modeled by a HKLM Hamiltonian with disorder and an

additional Dzyaloshinski-Moriya interaction. The role of these perturbations in driving the spin liquid behavior is unclear.^{7–10} On the theoretical side, a key problem is that there are no exact or nearly exact analytical or computational methods to solve infinite 2D quantum lattice systems. For one dimensional systems, the density matrix renormalization group^{11,12} (DMRG), the computational method used in this work, serves in this capacity. Another “Holy Grail” has been to find an accurate and widely applicable computational method for 2D many-body quantum systems.

The HKLM has been studied with approximate approaches by leading theorists for decades,¹³ with proposals for spin liquids and for valence bond crystals (VBCs).¹⁴ In the last few years some new numerical evidence has suggested that the HKLM ground state is *not* a spin liquid. Instead, calculations have indicated that it might be a VBC, with a large 36-site unit cell, called the honeycomb valence bond crystal (HVBC). First proposed by Marston and Zeng¹⁴, and explored in more detail by Nikolic and Senthil¹⁵, the HVBC was studied with a perturbative series expansion by Singh and Huse¹⁶, who found the series for the ground state energy to be rapidly converging and to give a low energy. Subsequently, Evenbly and Vidal utilized the multiscale entanglement renormalization ansatz (MERA) on the HKLM to obtain a similar estimate of the energy of the HVBC¹⁷. MERA is related to DMRG but can be implemented directly in 2D. This MERA study also produced the lowest numerically exact upper bound to the energy per site, which was close to the series expansion energy. A recent DMRG study¹⁸, in contrast, found a spin liquid ground state, but on the largest lattices the energy obtained was substantially above that of the HVBC, suggesting that the method had not found the true ground state.

Here we perform a much more extensive DMRG study of the HKLM with important differences in techniques

from the previous study. Most importantly, we avoid fully periodic (toroidal) boundary conditions, which are known to greatly magnify the truncation errors in DMRG compared to samples with open ends¹². We present compelling evidence that the ground state of the HKLM is a spin liquid. This spin liquid has an energy which is substantially below that of the HVBC. We also provide a new rigorous upper bound on the ground state energy of the infinite 2D system. The spin liquid ground state is gapped to both singlet and triplet bulk excitations, with short correlation lengths. The short correlation lengths make the finite circumference (up to 12 bond lengths) cylinders that we can study converge rapidly towards two dimensions both in energy and properties. The spin liquid resembles a Z_2 topologically-ordered short range resonating valence bond (RVB) state,^{19–22} but has significant internal structure with a key role apparently played by eight-site resonant loops.

II. DMRG METHODS

The density matrix renormalization group¹¹ is ideal for one dimensional systems, but also has long been used for finite-width 2D strips or cylinders^{23,24}. To maintain a constant accuracy as the width of the system is increased, the number of states kept per block m must increase exponentially, increasing the computer resources needed, and thus limiting the maximum width feasible. High accuracy is required to distinguish between phases in the KLHM, so we have limited the systems studied to a maximum circumference of 12 lattice spacings, for which we can obtain a relative error of less than 0.1% in extrapolated energy.

We use a cylindrical geometry for most of our calculations, which we label by the cylinder’s orientation and circumference. We put the circumference of the cylinder either along or close in orientation to the y -axis. For example, in our notation YC8 indicates a cylinder (C) in which one of the three bond orientations is along the y -axis (Y), and the circumference is 8 lattice spacings. For cylinders oriented with some bonds along the x -direction (X), the circumference is measured in units of $\sqrt{3}/2$ times the lattice spacing, so that XC8 has a circumference of $c = 4\sqrt{3}$ lattice spacings. For cylinders which connect periodically around the cylinder’s axis with a shift, the shift is added to the label: e.g. YC9-2 indicates a YC9 cylinder which is connected with a horizontal shift at the “seam” of two units; YC9-2 has a circumference of $c = 2\sqrt{21}$. In these cases with shifts the kagome lattice is wrapped on the cylinder in a spiral.

There are two key issues that complicate the calculations: 1) the geometry of the cluster—the circumference, the periodic shift, the boundary conditions at the open ends—can affect the ground and excited states significantly; and 2) on the wider systems, DMRG can get stuck in metastable states. Both of these problems can be surmounted, but it is necessary to study a wide variety

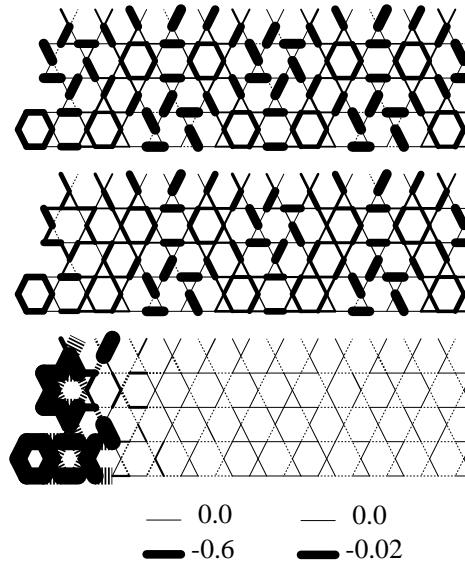


FIG. 1: Valence bond pattern for the left two-thirds of a 208 site XC8 cylinder. The width of the lines is proportional to $|\langle \vec{S}_i \cdot \vec{S}_j \rangle|$ (top two panels and left key) or $|\langle \vec{S}_i \cdot \vec{S}_j \rangle - e_\alpha|$ (bottom panel, right key), with dashed lines indicating the quantity is positive. Here α signifies bond direction and the approximate bulk bond correlations are $e_\alpha = -0.223$ for horizontal bonds and -0.217 for diagonal. The top panel shows sweep 6 with $m = 200$, the middle panel sweep 14 with $m = 600$, and the bottom panel the final sweep 34 with $m = 8000$. Near $m = 2400$ (not shown), the energy drops fairly abruptly by about 0.1%, and the HVBC is replaced by a spin liquid state. The line widths have been constrained to a maximum near the left edge, bottom panel.

of systems and initial states to find out which geometries do not frustrate the lowest energy states and how to prepare initial states which permit the algorithm to find the ground state. The results presented here are a very small fraction of the total number of systems studied, and have been selected to illustrate the key behavior most clearly.

III. THE VALENCE BOND CRYSTAL VERSUS THE SPIN LIQUID

In this section we present some of the key evidence that the ground state of the KLHM is a spin liquid, and specifically not the HVBC. To rule out the HVBC on the cylinders we have studied, despite the possibility of metastable states, a valuable technique is to favor the HVBC, both in initial state and boundary conditions. In spite of thus favoring it, the HVBC is unstable in the resulting simulations, which is strong evidence against an HVBC ground state. A typical example is shown in Fig. 1. In this simulation the cylinder circumference and wrapping vector accommodate the HVBC state, the left and right edges of the cluster were trimmed to accommodate and pin the HVBC state, the initial state was

prepared in the HVBC state, and the ordering of the sites of the cylinder used by the DMRG followed an irregular path which always makes any two sites sharing a valence bond in the HVBC adjacent. (This biased special ordering allows a perfect non-resonating HVBC to be represented keeping only $m = 2$ states per block.) These biases towards the HVBC state (particularly the ordering) make it metastable out to about $m = 2400$, after which it transitions to a spin liquid state. The irregular edges (along with a variety of other considerations) allow us to completely rule out the possibility that the uniform state is a superposition of shifted HVBCs. The final state is a remarkably uniform spin liquid in the center of the system, with only slight perturbations from the open, irregular edges and incomplete convergence, and a slight anisotropy from the finite circumference. This system clearly has a very small length scale for the decay of the perturbations due to the ends. If we use a more conventional ordering of sites, the HVBC is not even metastable; it disappears within the first few sweeps with $m < 200$. Energies are generally lower for a fixed m for the standard ordering than for the special ordering.

We do not find the HVBC to be the ground state on any of the cylinders we have studied. However, on the largest circumference cylinders, for which our accuracy is much reduced, the HVBC can be metastable even with the more unbiased standard site ordering. (A small bias is still present favoring the less entangled HVBC state.) For these systems we can compare energies between a prepared HVBC state and other states. Even in cases where the final energies are not accurate enough to clearly pick one state, we may be able to judge that the HVBC is not the ground state. In Fig. 2 we show such a case for a 400 site YC12 cylinder. Two runs were performed, one pinned to start as a HVBC, the other started with an essentially random initial state. Just after the pinning is released at $m = 600$, we see the HVBC has lower energy. However, near $m = 2000$ the initially random state is finding the spin liquid state and becomes lower in energy. Subsequently, the difference between the two energies widens as m is increased. The final state (not shown) appears to be a spin liquid with several localized defects which the simulation had not yet eliminated.

The series expansions of Singh and Huse¹⁶ treat the HVBC strong-bond interactions as having a fixed $J = 1$, while the weak bonds have their interactions modified by a factor λ ; the expansion is about $\lambda = 0$, and the uniform kagome lattice has $\lambda = 1$. We have studied the ground state along this path of modified Hamiltonians $H(\lambda)$ for a 194-site XC8 cylinder. Along this path the system has an apparent first-order phase transition near $\lambda_c = 0.984$. This transition is most clearly seen using a “hysteresis plot”. In Fig. 3 we show results from three different runs. Each run has a fixed m , and λ is changed between each DMRG sweep, with λ first increasing, then decreasing (note the arrows). The simulation cannot adapt the wavefunction from one phase to another in one sweep, so the system shows hysteresis, staying in the old higher en-

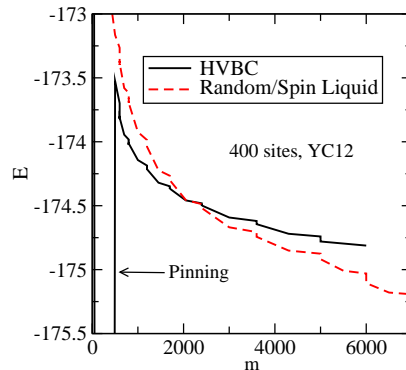


FIG. 2: Total energy E as the number of states kept m is increased for a 400 site YC12 cylinder, with two different initial states—one essentially random, the other with temporary pinning fields to force an HVBC.

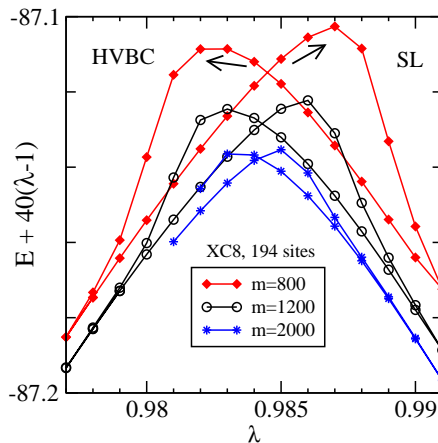


FIG. 3: Hysteresis plot for a 194 site XC8 cylinder showing the apparent first-order phase transition between valence bond crystal and spin liquid. For each of the three runs, the Hamiltonian parameter λ (see text) is changed for every DMRG sweep, thus tracing out a path through parameter space that resembles the time evolution of a system under changing λ . A linear approximation to the main trend of the energy E with λ has been subtracted out.

ergy state for several sweeps before drifting down to the new lower energy state. The crossing point of the curves in the two different directions converges very rapidly with increasing m to the transition point λ_c , even though the total energies have lower accuracy. This first-order transition shows why the series expansion converged so well,¹⁶ but to an energy that was not the ground state energy at $\lambda = 1$.

For any of the cylinder geometries we can obtain an estimate of the energy per site for the infinitely long cylinder by subtracting energies of cylinders of different length to eliminate end effects. The best results are obtained by doing a sequence of m values for each cluster and extrapolating in the truncation error. For $\lambda = 0.98$ on XC8, which is in the HVBC phase, we obtain an energy per

site of $-0.43237(4)$. This agrees fairly well with the series expansion energy for this cylinder and λ , $-0.431(1)$. This supports the idea that the series expansion gives a reasonable estimate of the energy of the HVBC phase at $\lambda = 1$ in two dimensions: $-0.433(1)$,¹⁶ as does the MERA HVBC energy, -0.4322 ,¹⁷ which is a rigorous upper bound. MERA produces a rigorous upper bound because it generates a wavefunction for the infinite 2D system and evaluates its energy exactly (up to floating point round-off errors).¹⁷

IV. GROUND STATE ENERGIES

It is possible to generate rigorous upper bounds on the ground state energy of the infinite 2D system from our results for finite open systems. Consider an open cluster C which can be “tiled” to fill all of 2D, with no sites left out, and having an even number of sites N_C . We take as a 2D variational ansatz a product wavefunction, the product being over all the tiles, where we use our best variational wavefunction for C (call it $|C\rangle$, with energy E_C) as the ansatz for each tile. The energy of any of the missing bonds connecting different tiles is zero, since $\langle C|\tilde{S}_i|C\rangle = 0$ for any spin i . Therefore the energy per site of this simple product wavefunction is E_C/N_C .

This approach is crude and converges slowly with the cluster size, with an error proportional to one over the width. Nevertheless, the SL energy is sufficiently low that we have been able to obtain a new rigorous upper bound on the 2D energy: $E_0^{(2D)} < -0.4332$. This was obtained with a width-12 open strip (which looks like XC12 unrolled) with $N_C = 576$, keeping $m = 5000$ states. The interior of this cluster had the uniform valence bond pattern expected for a spin liquid.

TABLE I: Ground state energies and gaps for infinitely long cylinders of various circumferences, c . The third column indicates whether the diamond pattern fits perfectly on the cylinder.

$(c/2)^2$	Cylinder	DF	E/N	Singlet Gap	Triplet Gap
3	XC4	no	-0.4445		
4	YC4	yes	-0.4467		
7	YC5-2	no	-0.43791	0.0108(1)	0.083(1)
9	YC6	no	-0.43914	0.0345(5)	0.142(1)
12	XC8	yes	-0.43824(2)	0.050(1)	0.1540(6)
13	YC7-2	no	-0.43760(2)	0.020(1)	0.055(4)
16	YC8	yes	-0.43836(2)	0.0497(6)	0.156(2)
19	XC10-1	no	-0.4378(2)		
21	YC9-2	no	-0.4377(2)	0.032(3)	0.065(5)
25	YC10	no	-0.4378(2)	0.041(3)	0.070(15)
28	XC12-2	yes	-0.4380(3)	0.054(9)	0.125(9)
36	YC12	yes	-0.4379(3)		

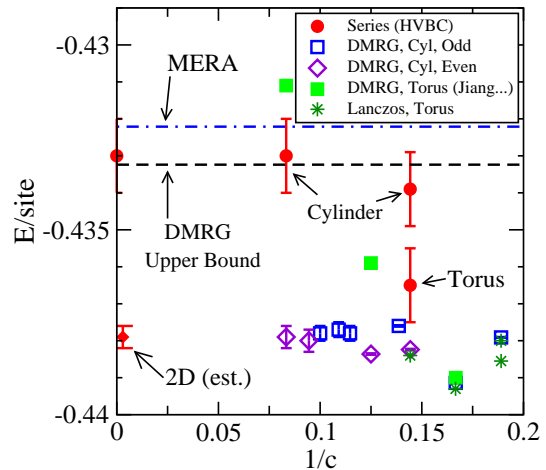


FIG. 4: Comparison of energies per site for various lattices and methods. For cylinders, the horizontal axis in this plot is the inverse circumference in units of inverse lattice spacings. For tori,^{18,25–27} the smallest circumference was used. In one case we show Lanczos energies for two different sized (36 and 42 sites) tori that have the same circumference.^{26,27} The MERA¹⁷ and our DMRG upper bound results apply directly to an infinite two dimensional system, as does the series HVBC result¹⁶ that is plotted on the axis. The torus DMRG energies¹⁸ are also upper bounds on the true ground state energies for those tori.

Our DMRG results are presented in Table I. The ground state energies are also plotted and compared to other calculations in Fig. 4. The DMRG energies are consistent with the Lanczos results^{25–27} and well below the energies of MERA¹⁷ and the series expansions for the HVBC.¹⁶ We note that the previous DMRG result¹⁸ is close to the true ground state²⁶ for the circumference 6 torus. The entanglement across a cut that separates a circumference 6 torus into two parts should be roughly the same as across a cut that separates a circumference 12 cylinder. We find that circumference 12 is presently our limit for obtaining good ground state energy estimates on cylinders. Thus it is perhaps not surprising that the DMRG results for tori¹⁸ give substantial overestimates of the ground state energies for circumferences larger than 6. But these estimates may alternatively be viewed as variational upper bounds obtained with DMRG.

The XC8 cylinder ($1/c \sim 0.14$) allows a direct comparison of the energies between the HVBC series and our DMRG: the DMRG energy is lower by $0.004(1)$, and the series result for XC8 is near the 2D result. The corresponding torus shows much larger finite size effects in the HVBC series,¹⁶ but the true finite size effects between the tori and cylinders are quite small, as seen by the nearly identical results from Lanczos on tori and DMRG on cylinders when we use the largest available torus at each circumference.^{25–27} This is consistent with the small correlation length apparent in Fig. 1. We conclude that our widest cylinders would have minimal finite size effects even if the system were in the HVBC phase; in the

spin liquid phase, the finite size effects for the energy are much smaller, and our ground state energies for the largest cylinders apply to 2D with minimal correction.

We now propose some nonrigorous bounds on the ground state energy of the infinite 2D system, by distinguishing between frustrated and unfrustrated cylinders. We call a cylinder unfrustrated if its ground state energy per site is lower than that of the 2D system. Here the periodic boundary conditions do not raise the ground state energy. Clearly, most of the very narrow cylinders have low energy (except possibly YC5-2), presumably due to the contribution to the energy from short RVB resonance paths that wind around the cylinder. We also believe that the “even” cylinders that are compatible with the 12-site unit cell diamond pattern that we discuss below are unfrustrated. Thus we propose that the energy of the XC8 cylinder provides a nonrigorous lower bound of -0.4382 per site on the 2D ground state energy. This cylinder has the same circumference as the 36-site torus that is the “standard” exact diagonalization cluster (torus). This “XC8” torus has ground state energy -0.43838 per site,²⁵ which is $0.00014(2)$ lower than the XC8 cylinder. The XC8 cylinder has only $1/3$ as many extra winding resonant paths as does the torus, so should have a correspondingly smaller finite-size effect in its ground state energy.

We believe that we also have at least one case (and probably many) of a cylinder that is frustrated, with a ground state energy above that for 2D. The argument for this also starts with the XC8 cylinder. Then we cut out a section of this cylinder with 42 sites and connect it to make a torus. This torus has various different new circumferences (topologically nontrivial ways to travel around it), which include YC7-2 and XC10-1. We sent this new (42-site!) torus out for exact diagonalization to Andreas Lauchli who promptly found its ground state energy, which is approximately 0.0001 per site *higher* than that of the XC8 cylinder.²⁶ From this we conclude that one or both of the new circumferences YC7-2 and XC10-1 must be frustrating to the spin liquid ground state and thus that cylinder should have a higher energy than the 2D system. This provides a nonrigorous upper bound on the 2D ground state energy of -0.4376 . Thus our current estimate of the 2D energy per site is

$$E_0^{(2D)} = -0.4379(3) .$$

Note that all the cylinders wider than YC8 have the same energy within the uncertainties, and thus rather small finite-size effects on their ground state energies.

V. THE STRUCTURE OF THE SPIN LIQUID GROUND STATE

The spin liquid ground state that we find has only short-range correlations and its ground state energy converges rapidly for finite circumference cylinders. We also find, as we discuss below, that there is a nonzero energy

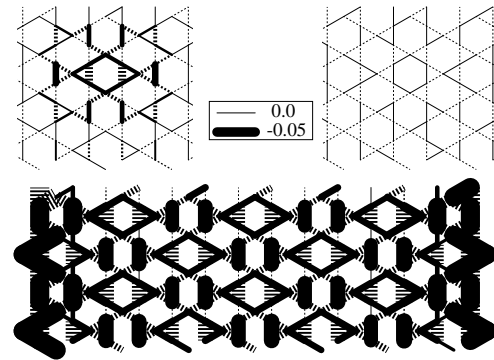


FIG. 5: Response of the spin liquid to small perturbations on cylinder YC8. In each case certain bonds have been strengthened: upper left, an 8 site diamond by 1%; upper right, a 6 site hexagon by 1%; and bottom, the wide strong and weak vertical bonds (28 of each) by $\pm 0.5\%$. Line widths indicate subtracted bond correlations, as in Fig. 1, bottom panel. Surrounding dimers arise in response to the diamond pinning in the upper left panel; the diamonds arise in response to dimer pinning in the lower panel.

gap for any excitations, including spin-singlet excitations. The structure of this ground state is apparently some sort of short-range resonating-valence-bond (RVB) state.²² The smallest resonant loops of singlet dimers in a nearest-neighbor RVB state on a kagome lattice each surround only one of the hexagons of the lattice. The possibilities are tabulated in, e.g., Table I of Nikolic and Senthil.¹⁵ If the RVB state had all dimer covers equally weighted, all 32 of these elementary loops would be equally present. What we find is that the ground state instead appears to substantially overweight certain 8-site loops of a diamond (or rhombus) shape. We first noticed this in seeing what patterns are easily produced in response to the details of how the samples are cut off at the ends.

To test the response of the ground state to enhancing each of these elementary resonant loops, we slightly increased the exchange couplings along the bonds of such a loop at the center of a YC8 cylinder, and saw how much this enhanced the spin-spin correlations along the loop and elsewhere. It is the 8-site diamond loop that elicits the strongest response, as is shown in Fig. 5. The 6-site “perfect hexagon” loop that has received attention in previous papers¹⁴⁻¹⁶ shows a much smaller response, suggesting that this resonant loop is actually underweighted in the RVB ground state.

One can not tile a kagome lattice with just these favored resonant diamonds. However, a particular “diamond pattern” valence bond crystal, shown in Fig. 5, appears to be closely related to the spin liquid, and it is useful to think of the spin liquid as a melted state of this crystal. One must keep in mind that the actual overlap of this state with the spin liquid is still small and the fluctuations are large. We have measured the correlation length for VBC correlations in this diamond pattern along cylinder YC8 and find that it is less than 1.5

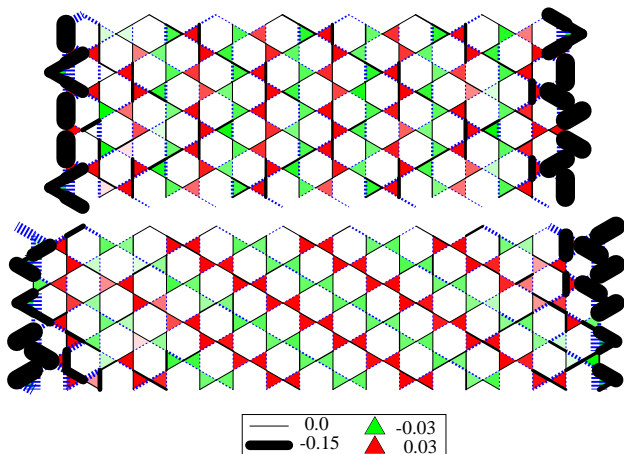


FIG. 6: Ground state energy patterns for a YC10 (top) and a YC9-2 cylinder. The colors of the triangles, and their intensities, indicate the deviation of the sum of the spin-spin correlations on the three bonds forming the triangle from $3e_0$, where we take $e_0 = -0.219$.

lattice spacings. Unlike the HVBC, this diamond VBC evolves smoothly into the spin liquid without any phase transition as one changes the strengths of the exchanges appropriately to favor it (we call this “pinning it”). For the even cylinders on which this diamond VBC does fit, this is very useful, as it allows a careful production of the spin liquid, by approaching it in a controlled and smooth fashion from this diamond VBC.

This diamond pattern was essential in extracting our most accurate ground state energy estimate for YC12. Applying the pinning pattern of the lower panel of Fig. 5 reduces the entanglement of the resulting state, allowing us to obtain more accurate energies. The pinning applies an equal number of positive and negative terms, so the energy dependence on the pinning coefficient η has no linear term near $\eta = 0$ for the uniform spin liquid. After verifying this on several cylinders and determining that a nearly pure quadratic behavior held for $\eta \leq 0.02$, we extrapolated $E(\eta)$ using the simple formula $E(0) = 4/3E(0.01) - 1/3E(0.02)$. This procedure reduced our energy uncertainty for YC12 by a factor of about 5. (The standard approach of simply extrapolating to zero truncation error at zero pinning gave $-0.4375(14)$.)

The infinitely long cylinders may be viewed as one-dimensional systems with a unit cell containing multiple spins. For those “even” cylinders that are compatible with the diamond VBC, this unit cell contains an even number of spins (e.g., for YC8 it contains 12 spins). In these cases the ground state of the infinite cylinder appears to be nondegenerate and gapped. But for the “odd” cylinders that are not compatible with the diamond VBC, the unit cell contains an odd number of spins, and the Lieb-Schultz-Mattis theorem says the ground state must be degenerate.²⁸ We find that the ground states on these odd cylinders weakly break trans-

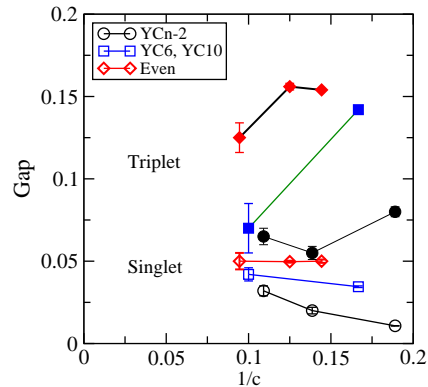


FIG. 7: Spin triplet (solid symbols) and singlet (hollow symbols) gaps for various cylinders with circumferences c .

lational invariance, spontaneously doubling the unit cell, and this produces a pair of degenerate ground states, still with a gap to higher excited singlet states. The symmetry breaking is in a “striped” pattern that is shown in Fig. 6. For YC6 and YC10 the stripes run around the circumference, while for the other odd spiral cylinders the stripes are spirals.

VI. GAPS

To explore the low-lying excited states on our cylinders we use the following DMRG procedure: first target only one state, and sweep enough to obtain a high-accuracy ground state. Then restrict the range of bonds which are updated in the DMRG sweeps to the central half of the sample, and now target the two lowest-energy states, again sweeping to high accuracy, but keeping the end regions of the samples locally in the ground state. This restricted sweeping prevents the low-lying excitations from being bound to the ends of the sample. This technique is particularly important for obtaining the singlet gap. For the triplet gap, we can also apply magnetic fields on the ends to prevent any edge excitations from appearing and hiding the bulk gap. For the triplet, we can also target both states together, one with total $S_z = 0$ and the other with $S_z = 1$, or run the two states separately. These different approaches allowed for fairly independent checks on the results; in addition, we also varied the lengths and how quickly the number of states kept was increased. The results for these gaps are presented in Table I. Getting gaps is more demanding than getting ground state energies, so our gap estimates do not go to as wide cylinders as do our ground state estimates.

Our gap results for the singlet and triplet gaps differ in an interesting way from what is known about the gaps from exact diagonalization.^{25,29}

We believe that we have found good evidence for a nonzero singlet gap of about 0.04 or 0.05 in the 2D system. This is quite different from the exact diagonalization results, where there are many lower-lying singlets,

and the lowest singlet gap is only about 0.01 on the 36-site torus.²⁹ As can be seen in Table I, the singlet gap is 0.050, within the errors, for the even XC8 and YC8 cylinders, and it remains near this value, although with much larger uncertainty, for the wider even XC12-2 cylinder. The odd cylinders, on the other hand, have smaller singlet gaps that increase as the circumference is increased, as shown in Fig. 7. The odd cylinders come in at least two “families”: YC6 and YC10 are not spirals, while YC5-2, YC7-2 and YC9-2 are a series of spirals with increasing circumference. In each of these (short) sequences of odd cylinders the singlet gap increases as the circumference increases, supporting our conclusion that the singlet gap remains nonzero in the 2D limit.

The triplet (spin) gap on the standard 36-site torus is 0.164 from exact diagonalization.²⁵ While XC8 and YC8 have gaps which are quite close to this, our results on other cylinders suggest that the two dimensional triplet gap is much smaller, as can be seen from Fig. 7. The triplet excitations appear to be composed of two spinons, but we cannot resolve whether or not the two spinons bind, although in some cylinders any binding must be very weak. This composite nature of the excitation seems to make the finite size effects and variation between the cylinders more pronounced. We do not yet understand the details of these effects. As in the singlet gap, the spiral odd cylinders have the smallest gaps, and the even the largest. Note that the triplet gap remains above the singlet gap in the systems we have studied, and we believe it remains nonzero in the 2D limit.

VII. INDICATIONS OF Z_2 TOPOLOGICAL ORDER

A nearest-neighbor RVB wavefunction is a linear combination of nearest-neighbor singlet dimers covering the kagome lattice.²² For a kagome lattice wrapped on a cylinder, like we are studying, such dimer covers are in two topologically distinct classes, and dimer resonances on finite loops remain in the same topological sector.^{21,22} We can force our samples to be in one or the other of these two topological sectors by choosing how many spins to leave at each end. An example of this is apparent for the YC10 cylinder in Fig. 6, where we force the pattern by the number of spins we leave “sticking out” at each end. For odd cylinders, the two sectors are related by translation along the length of the cylinder, so are degenerate. For even cylinders, on the other hand, the finite circumference c allows the two sectors to have different ground state energies. The difference in energy per site should vanish as $\sim \exp(-c/\xi)$, where ξ is a correlation length. We can measure this splitting for YC8, where it is 0.00069(3) per site, but for the wider even cylinders we do not yet have an estimate, because it is more difficult to get a reliable ground state in the higher-energy topological sector. It is also worth noting that on XC8 and YC8 the singlet gap above the higher-energy topological

ground state is substantially smaller than the singlet gap above the overall ground state, which is presumably a factor in making the higher-energy sector more difficult to work with in DMRG.

A domain wall along the cylinder between regions in the two different topological ground states is a spinon. For the odd cylinders, the degeneracy of the two topological sectors means the spinons are unconfined. However, two spinons might bind with a finite binding energy: it appears that this might be happening on cylinder YC10 and thus it might also occur in the 2D limit. For the even cylinders, on the other hand, the spinons are confined by an effective potential that grows linearly with the distance, because the domain between them is in the higher-energy topological state. As a result, the excitation across the spin gap for the even cylinders must be a bound spinon pair. It remains to be determined if they remain bound in the 2D limit.

We suspect that the lowest-lying “bulk” singlet excitations that we obtain are bound pairs of visons. It will be interesting to try to test this idea by attempting to pull apart such a vison pair or to try make a single vison near the end of a cylinder, but this remains for future research.

VIII. CONCLUSIONS

Using very accurate DMRG methods we have found a spin liquid ground state for the HKLM on cylinders with circumference up to 12 lattice spacings. The energies are much lower than for the competing valence bond crystal state. The combination of low energies and small finite size effects due to short correlation lengths and nonzero singlet gaps, a new rigorous energy bound, and a simple picture for the nature of the spin liquid provide compelling evidence that the infinite 2D system is a gapped RVB-like spin liquid. Much remains to be understood concerning this phase, particularly the detailed structure, exchange statistics and dispersion relations of the various excitations. It should also be instructive to explore the phase diagram in the vicinity of this simple nearest-neighbor-only Heisenberg model by changing the Hamiltonian in various ways in order to find what other phases are nearby and perhaps to move “deeper” into this spin liquid where it might be easier to study.

We thank Andreas Lauchli for sending us numerous new exact diagonalization results. We thank Rajiv Singh for explaining how to convert the published series results for the 36-site torus and the 2D system to results for cylinders. We thank Claire Lhuillier for suggesting displaying the energies of the triangles, as in Fig.6. We also thank them all again, as well Matthew Fisher, T. Senthil, Erik Sorensen, Shivaji Sondhi, Guifre Vidal, Xiao-gang Wen, Oleg Tchernyshyov and Miles Stoudenmire for helpful discussions. We acknowledge the support of the NSF under grants DMR-0907500 and DMR-0819860.

-
- ¹ L. Balents, *Nature* **464**, 199 (2010).
² P. W. Anderson, *Science* **235**, 1196 (1987).
³ L. B. Ioffe, M. V. Feigel'man, A. Ioselevich, D. Ivanov, M. Troyer and G. Blatter, *Nature* **415**, 503 (2002).
⁴ M. Kohno, O. A. Starykh and L. Balents, *Nat. Phys.* **3**, 790 (2007).
⁵ Z. Y. Meng, T. C. Lang, S. Wessel, F. F. Assaad and A. Muramatsu, *Nature* **464**, 847 (2010).
⁶ G. Misguich, B. Bernu, C. Lhuillier and C. Waldtmann, *Phys. Rev. Lett.* **81**, 1098 (1998).
⁷ P. Mendels, *et al.*, *Phys. Rev. Lett.* **98**, 077204 (2007).
⁸ J. S. Helton, *et al.*, *Phys. Rev. Lett.* **98**, 107204 (2007).
⁹ O. Ofer, *et al.*, *cond-mat/0610540*.
¹⁰ T. Imai, E. A. Nytko, B. M. Bartlett, M. P. Shores and D. G. Nocera, *Phys. Rev. Lett.* **100**, 077203 (2008).
¹¹ S. R. White, *Phys. Rev. Lett.* **69**, 2863 (1992).
¹² S. R. White, *Phys. Rev. B*, **48**, 10345 (1993).
¹³ V. Elser, *Phys. Rev. Lett.* **62**, 2405 (1989).
¹⁴ J. B. Marston and C. Zeng, *J. Appl. Phys.* **69**, 5962 (1991).
¹⁵ P. Nikolic and T. Senthil, *Phys. Rev. B* **68**, 214415 (2003).
¹⁶ R. R. P. Singh and D. A. Huse, *Phys. Rev. B* **76**, 180407 (2007); *ibid.*, **77**, 144415 (2008).
¹⁷ G. Evenbly and G. Vidal, *Phys. Rev. Lett.* **104**, 187203 (2010).
¹⁸ H. C. Jiang, Z. Y. Weng and D. N. Sheng, *Phys. Rev. Lett.* **101**, 117203 (2008).
¹⁹ P. W. Anderson, *Mater. Res. Bull.* **8**, 153 (1973).
²⁰ X. G. Wen, *Phys. Rev. B* **44**, 2664 (1991).
²¹ R. Moessner and S. L. Sondhi, *Phys. Rev. Lett.* **86**, 1881 (2001).
²² G. Misguich, D. Serban and V. Pasquier, *Phys. Rev. Lett.* **89**, 137202 (2002).
²³ S. R. White and D. J. Scalapino, *Phys. Rev. Lett.* **80**, 1272 (1998).
²⁴ S. R. White and A. L. Chernyshev, *Phys. Rev. Lett.* **99**, 127004 (2007).
²⁵ P. W. Leung and V. Elser, *Phys. Rev. B* **47**, 5459 (1993).
²⁶ A. M. Lauchli [private communication].
²⁷ E. S. Sorensen [private communication].
²⁸ E. Lieb, T. Schultz and D. Mattis, *Ann. Phys.* **16**, 407 (1961).
²⁹ C. Waldtmann, *et al.*, *Eur. Phys. J. B* **2**, 501 (1998).

